BULLETIN OF ENGINEERING SCIENCE, TECHNOLOGY AND INDUSTRY
(BESTI Journal) | ISSN (e): 3025-5821
Website : https://bestijournal.org/index.php/go/index | Volume 4 No. 3 (2026)

THE EFFECT OF TILT ANGLE AND MOUNTING HEIGHT ON BIFACIAL GAIN AND ANNUAL ENERGY YIELD OF A ROOFTOP BIFACIAL PV SYSTEM: A PVSYST PARAMETRIC ANALYSIS IN THE HUMID TROPICAL CLIMATE OF SOUTH SULAWESI

Heriani[1]*, Muhammad Iqbal Nikmatullah[2]
Department of Marine Engineering, Faculty of Engineering, Hasanuddin University, Gowa, South Sulawesi
Department of Marine Engineering, Faculty of Engineering, Hasanuddin University, Gowa, South Sulawesi
E-mail: heriani21d@student.unhas.ac.id [1]*, lakibbal@unhas.ac.id [2]

Received: 24/06/2026 | **Revised:** 05/07/2026 | **Accepted:** 27/07/2026 | **Published:** 11/08/2026

Abstract

Bifacial photovoltaic (PV) modules capture solar irradiance on both front and rear surfaces, with the rear-side contribution quantified as bifacial gain (BG), highly sensitive to tilt angle and mounting height above the roof surface. A systematic simulation study simultaneously varying both parameters for the humid tropical climate of South Sulawesi, Indonesia has not been found in publicly indexed databases (Google Scholar, Scopus, SINTA, Garuda, Neliti; last searched 10 June 2025). This study presents a parametric simulation dataset through 20 PVsyst 7.3.1 variants combining five tilt angles (5–25°) with four mounting heights (0.30–1.00 m) for a 10.8 kWp grid-connected bifacial rooftop system (5.2334°S, 119.5047°E; GHI = 1,855 kWh/m²/yr). Results show tilt 10° consistently maximizes annual energy yield (E_grid) across all heights, consistent with low-latitude theory and field measurements by Khoo et al. (2014), peaking at 17,631 kWh/yr (PR = 0.871; BG = 8.0%) at H = 1.00 m. Albedo sensitivity analysis shows BG ranging 6.1–10.2% across albedo 0.15–0.30, with a disproportionate +2.2 pp increase at the 0.25→0.30 step, consistent with the nonlinear albedo–BG relationship reported by Deline et al. (2020), though the underlying mechanism requires field confirmation. This study is a simulation-based parametric analysis without on-site field validation, a limitation stated explicitly throughout; results should not be treated as experimentally validated values.

Keywords: bifacial gain, bifacial photovoltaic, mounting height, tilt angle, tropical climate

INTRODUCTION

Indonesia is accelerating its transition toward renewable energy while meeting continuously increasing electricity demand. Government Regulation No. 79 of 2014 targets a renewable energy contribution of 23% by 2025 (Government of the Republic of Indonesia, 2014). Owing to its equatorial location, Indonesia possesses abundant solar resources with an average global horizontal irradiance (GHI) of 4.5–5.1 kWh/m²/day (Ministry of Energy and Mineral Resources, 2020). The southern part of South Sulawesi (5.2334°S, 119.5047°E), which is the focus of this study, has an annual GHI of approximately 1,855 kWh/m²/year based on Meteonorm 8.0 data (Remund et al., 2020), exceeding the solar resource reported for Singapore (Khoo et al., 2014). These favorable conditions make rooftop photovoltaic (PV) systems an attractive solution for sustainable electricity generation.

Among current PV technologies, bifacial modules have attracted considerable attention because they generate electricity from both the front and rear surfaces. While the front side receives direct and diffuse irradiance, the rear side captures reflected radiation from the surrounding surface (albedo) and diffuse sky irradiance, thereby increasing the overall energy yield. This additional contribution is commonly expressed as bifacial gain (BG), which generally ranges from 3–15% depending on installation conditions (Marion et al., 2017; Sun et al., 2018). Previous studies have shown that BG is primarily influenced by three installation parameters: tilt angle, mounting height, and surface albedo, whose interaction is governed by the geometric view-factor mechanism (Appelbaum & Bany, 1979; Asgharzadeh et al., 2018; Deline et al., 2020).

A literature survey conducted through Google Scholar, Scopus, SINTA, Garuda, and Neliti (last searched 10 June 2025) found no indexed study simultaneously investigating tilt angle and mounting height for rooftop bifacial PV systems under the humid tropical climate of South Sulawesi. Although Khoo et al. (2014) investigated optimal tilt angles in Singapore using field measurements, their work focused on monofacial systems and emphasized orientation rather than bifacial performance. Sun et al. (2018) evaluated mounting-height effects on bifacial systems under temperate climatic conditions, while other studies generally examined only individual installation parameters or different climatic environments (Asgharzadeh et al., 2018; Deline et al., 2020). Consequently, practical design guidance for rooftop bifacial PV systems in humid tropical regions with annual GHI exceeding 1,800 kWh/m²/year remains limited.

To address this gap, this study performs a parametric simulation using PVsyst 7.3.1 by simultaneously varying tilt angle (5°–25°) and mounting height (0.30–1.00 m) for a 10.8 kWp grid-connected rooftop bifacial PV system in South Sulawesi. The objectives are to (1) evaluate the combined effects of tilt angle and mounting height on annual energy yield (E_grid) and bifacial gain (BG); (2) identify the configuration that maximizes annual energy production and bifacial performance; and (3) assess the sensitivity of system performance to variations in albedo and bifaciality factor. The principal contribution of this study is a systematic parametric dataset that provides engineering design recommendations for rooftop bifacial PV installations in humid tropical climates. The study is explicitly presented as a numerical simulation using PVsyst without field validation, following established simulation frameworks reported in previous studies (Sun et al., 2018; Deline et al., 2020; Asgharzadeh et al., 2018).

LITERATURE REVIEW

2.1 Bifacial Panel Technology, Bifacial Gain, and Bifacial Performance Ratio

A bifacial PV module is a module whose solar cells are active on both sides, enabling energy conversion from irradiance received at both the front and rear surfaces (Kopecek & Libal, 2021). The key parameter distinguishing bifacial modules is the bifaciality factor (φ), defined by IEC TS 60904-1-2:2019 (International Electrotechnical Commission [IEC], 2019) as the ratio of rear-side to front-side conversion efficiency under identical STC irradiance, generally ranging from 0.65–0.85 for commercial modules. The LONGi Solar LR5-72 HIBD 540 Wp module used in this study has φ = 0.70 according to its official datasheet.

Bifacial Gain (BG)

Bifacial gain is defined as the percentage increase in energy of a bifacial system relative to a reference monofacial system under identical installation conditions, following IEC TS 60904-1-2:2019 (IEC, 2019):

$$BG\ (\%) = [(E_0\_bifacial - E_0\_monofacial) / E_0\_monofacial] \times 100\% \quad (1)$$

where E_0_bifacial and E_0_monofacial are, respectively, the annual energy of the bifacial system and the reference monofacial system under identical installation conditions (Marion et al., 2017). In the PVsyst simulation, BG is obtained directly from the Loss Diagram as the percentage contribution of rear-side irradiance to the total effective irradiance, as described in the PVsyst version 7.x technical documentation

Bifacial Performance Ratio (BPR)

BPR is defined as the ratio of actual energy yield to the energy that would be produced if the system were irradiated entirely at the effective bifacial irradiance, consistent with the definition used by Deline et al. (2020) and Mermoud & Lejeune (2010):

$$BPR = E\_yield / (G\_eff\_bif \times P\_STC / G\_STC) \quad (2a)$$

where E_yield is the actual energy delivered to the grid (kWh/year), G_eff_bif is the effective bifacial irradiance on the collector plane (kWh/m²/year) = G_front + φ × G_rear, P_STC is the system's nominal capacity (kWp), and G_STC = 1 kWh/m² is the STC reference irradiance. An equivalent form using module parameters is:

$$BPR = E\_yield / (G\_eff\_bif \times A \times \eta\_STC) \quad (2b)$$

where A is the total module area (m²) and η_STC is the module efficiency at STC. The two forms are equivalent because P_STC = A × η_STC × G_STC. Because G_eff_bif is greater than G_front alone (a larger denominator), BPR values are consistently lower than the standard PR. BPR is a more comprehensive metric for bifacial systems than the standard PR because it accounts for the rear-side contribution in the denominator.

Numerical Verification of BPR (Tilt 10°, H = 1.00 m)

The internal consistency of the BPR definition can be verified using the data in Table 1 (Tilt 10°, H = 1.00 m row) — see Section 4.1. From E_grid = 17,631 kWh/year, PR = 0.871, and P_STC = 10.8 kWp, the effective frontal irradiance (G_front) is obtained from the standard PR definition (IEC, 2021):

$$G\_front = E\_grid / (PR \times P\_STC) = 17{,}631 / (0.871 \times 10.8) = 1{,}873.8 \text{ kWh/m}^2\text{/year} \quad (V1)$$

Since BG = 8.0% indicates that the rear-side contribution to G_front is 8.0%, the effective bifacial irradiance is:

$$G\_eff\_bif = G\_front \times (1 + BG/100) = 1{,}873.8 \times 1.080 = 2{,}023.7 \text{ kWh/m}^2\text{/year} \quad (V2)$$

Substituting into Equation (2a) yields:

$$BPR = 17{,}631 / (2{,}023.7 \times 10.8) = 0.806 \approx 0.805 \quad (V3)$$

The resulting BPR = 0.806 is consistent with the value in Table 1 (BPR = 0.805) within the rounding margin of the intermediate calculations, confirming the internal consistency between Equation (2a), the simulation data in Table 1, and the BG definition used by PVsyst.

Performance Ratio (PR) and Specific Yield (Yf)

The PV system Performance Ratio is defined by IEC 61724-1:2021 (IEC, 2021) as:

$$PR = Yf / Yr \quad (3a)$$

$$Yf = E\_grid / P\_nom \quad (3b)$$

where Yf (final yield, kWh/kWp/year) is the specific actual energy yield, Yr (reference yield, kWh/kWp/year) is the annual irradiation on the collector plane divided by 1 kW/m² (STC irradiance), E_grid is the energy injected into the grid (kWh/year), and P_nom is the system's nominal capacity at STC (kWp) (IEC, 2021).

2.2 View Factor Model and the Influence of Installation Geometry

The view factor (VF) is a geometric parameter that defines the fraction of radiation emitted from one surface and received by another. Appelbaum and Bany (1979) derived the view-factor equations for panel-array configurations.

Rear-Side View Factor (Appelbaum & Bany)

For an unlimited-sheds-type system with tilt angle β, and for a single row without shading effects from a preceding row, the rear-side view factor toward the sky and the ground is expressed as (Appelbaum & Bany, 1979):

$$VF\_rear{\rightarrow}sky = (1 - \cos\beta) / 2 \quad (4a)$$

$$VF\_rear{\rightarrow}ground = 1 - VF\_rear{\rightarrow}sky = (1 + \cos\beta) / 2 \quad (4b)$$

For multi-row arrays with pitch p and panel height h above the ground, the shading contribution from the preceding row must be subtracted. Appelbaum and Bany (1979) showed that VF_rear→ground increases monotonically with h and behaves non-linearly with respect to β. The 2D Unlimited Sheds model implemented in PVsyst computes rear-side irradiance separately for the ground-reflected beam, ground-reflected diffuse, and direct sky-diffuse components — it does not explicitly model multi-bounce inter-reflection; the ground-reflection contribution is computed through a one-way view factor rather than iterative repeated reflection (Mermoud & Lejeune, 2010; Asgharzadeh et al., 2018).

Rear-Side Irradiance from Ground Reflection

The rear-side irradiance component originating from ground reflection is expressed by Marion et al. (2017) as:

$$G\_rear{,}ground = \rho \times G\_H \times VF\_rear{\rightarrow}ground \quad (5)$$

where ρ is the surface albedo (dimensionless), G_H is the global horizontal irradiance at the ground surface (W/m²), and VF_rear→ground is the geometric view factor from the panel's rear side to the ground (dimensionless) (Marion et al., 2017). Equation (5) shows that the relationship between albedo and G_rear,ground is directly linear; however, the response of BG to albedo can be non-linear because VF_rear→ground is itself a non-linear function of geometry (β and H), and because G_H is a component that depends on atmospheric conditions rather than being a constant. The explanation for the observed non-linearity is discussed further in Section 4.5.

2.3 Effect of Albedo and Its Non-Linear Nature

Surface albedo is the second most sensitive parameter (after mounting height) in determining bifacial gain. Albedo values vary significantly by material: fresh concrete 0.25–0.35; weathered concrete 0.15–0.25; asphalt 0.05–0.10; white paint 0.60–0.80 (Ineichen et al., 1990; Andrews & Pearce, 2013). Deline et al. (2020) showed that an albedo increase of 0.10 can raise BG by 2–4 percentage points depending on the system's geometric configuration. The relationship between albedo and BG is non-linear because the VF_rear→ground term in Equation (5) is a non-linear function of installation geometry, so the response of G_rear,ground to changes in ρ varies depending on the specific geometric operating point (Appelbaum & Bany, 1979; Deline et al., 2020).

2.4 Sensitivity to the Bifaciality Factor (φ)

The bifaciality factor φ is a module characteristic parameter set by factory testing and may vary within the specification range (0.65–0.75 for similar modules, per the IEC TS 60904-1-2:2019 tolerance (IEC, 2019)). The effect of φ on G_eff_bif is derived from the definition G_eff_bif = G_front + φ × G_rear (Marion et al., 2017). A change in φ of Δφ — with G_rear assumed unchanged — yields:

$$\Delta G\_eff\_bif = \Delta\varphi \times G\_rear \quad (6a)$$

The resulting change in BG, using a first-order linear approximation valid for small Δφ variations around the nominal φ value, is:

$$\Delta BG \approx (\Delta\varphi \times G\_rear \,/\, G\_front) \times 100\% \quad (6b)$$

The ratio G_rear/G_front is derived from the BG definition: BG (%) = φ × G_rear/G_front × 100% (IEC, 2019), so that:

$$G\_rear \,/\, G\_front = BG \,/\, (100 \times \varphi) \quad (6c)$$

At the optimal configuration (Tilt 10°, H = 1.00 m) with BG = 8.0% and φ = 0.70:

$$G\_rear \,/\, G\_front = 8.0 \,/\, (100 \times 0.70) = 0.114 \quad (6d)$$

For Δφ = ±0.07 (±10% of φ = 0.70), substituting into Equation (6b) gives:

$$\Delta BG \approx \pm 0.07 \times 0.114 \times 100\% = \pm 0.8 \text{ pp} \quad (6e)$$

This means that if the actual φ = 0.63 (lower ±10% bound), BG is estimated to drop by ~0.8 pp to ~7.2%; if φ = 0.77 (upper bound), BG rises by ~0.8 pp to ~8.8%. The ratio G_rear/G_front = 0.114 is derived from the simulation data and the nominal φ value, not measured directly from the Loss Diagram, and therefore carries the assumption that the internal irradiance distribution is consistent with PVsyst's BG definition. The sensitivity to φ (±0.8 pp) is smaller than the sensitivity to albedo (a range of 4.1 pp for albedo 0.15–0.30), confirming that albedo is the dominant source of uncertainty. Equation (6b) applies only to small Δφ variations around the nominal value; larger variations must be quantified through direct PVsyst simulation.

METHOD

3.1 Location and Meteorological Data

The simulation was carried out for a location at coordinates 5.2334°S and 119.5047°E (elevation 23 m a.s.l.), the actual coordinates used in PVsyst 7.3.1 during the simulation process. This location lies in the southern part of South Sulawesi, within a humid tropical climate zone. Meteorological data were obtained from Meteonorm version 8.0, based on the 2010–2014 period database with a 100% satellite-data saturation level (Remund et al., 2020). The authors acknowledge that the 2010–2014 data are more than a decade old; the use of Meteonorm 8.2 or 9.0, or actual BMKG (Indonesian Agency for Meteorology, Climatology, and Geophysics) measurement data, is recommended for future research. The principal climate parameters generated by Meteonorm 8.0 for this location are: annual GHI = 1,855 kWh/m²/year; average air temperature = 26.8°C; average wind speed = 3.2 m/s.

3.2 PV System Specification

The PV system consists of 20 LONGi Solar LR5-72 HIBD 540 Wp monocrystalline bifacial modules arranged in a 2 string × 10 module in series configuration, with a nominal capacity of 10.8 kWp (STC). The module's technical specifications, per its official datasheet, are: P_mpp = 540 Wp; V_mpp = 41.2 V; I_mpp = 13.1 A; V_oc = 49.8 V; I_sc = 13.9 A; efficiency = 20.93%; φ = 0.70. A Huawei SUN2000-10KTL-M1 inverter with a capacity of 10.0 kW_ac, an MPPT voltage range of 140–980 V, and 2 MPPT trackers is used. The baseline surface albedo is 0.25 (weathered concrete, per Ineichen et al. (1990)). The overall system configuration and DC–AC power flow are shown in Figure 1 and the electrical single-line diagram is presented in Figure 2.

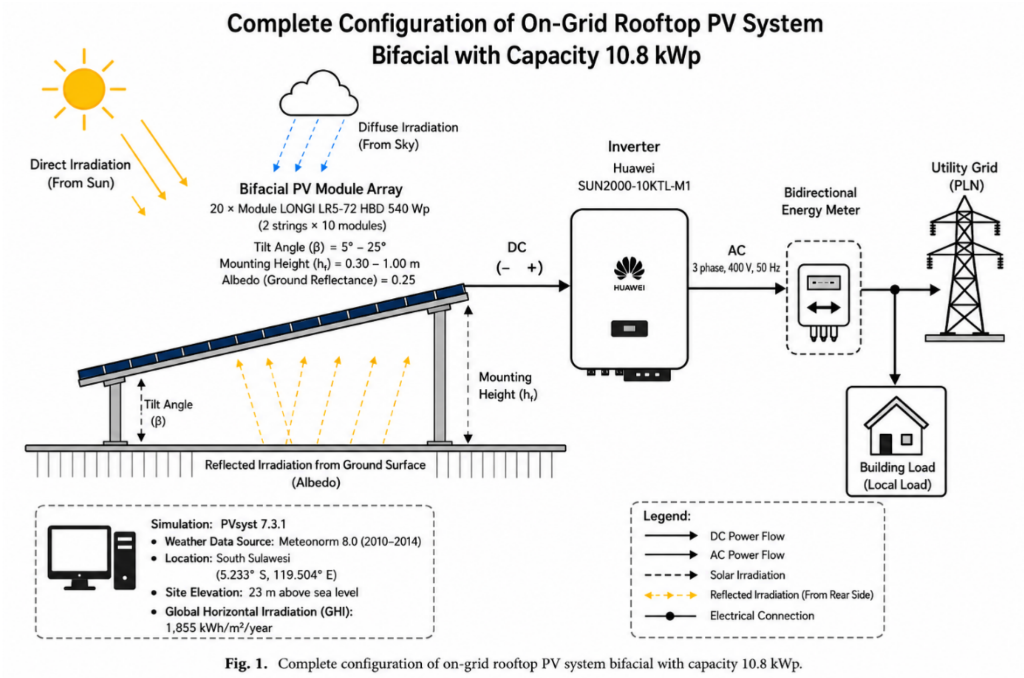

Figure 1. Overall Configuration of the 10.8 kWp On-Grid Bifacial Rooftop PV System

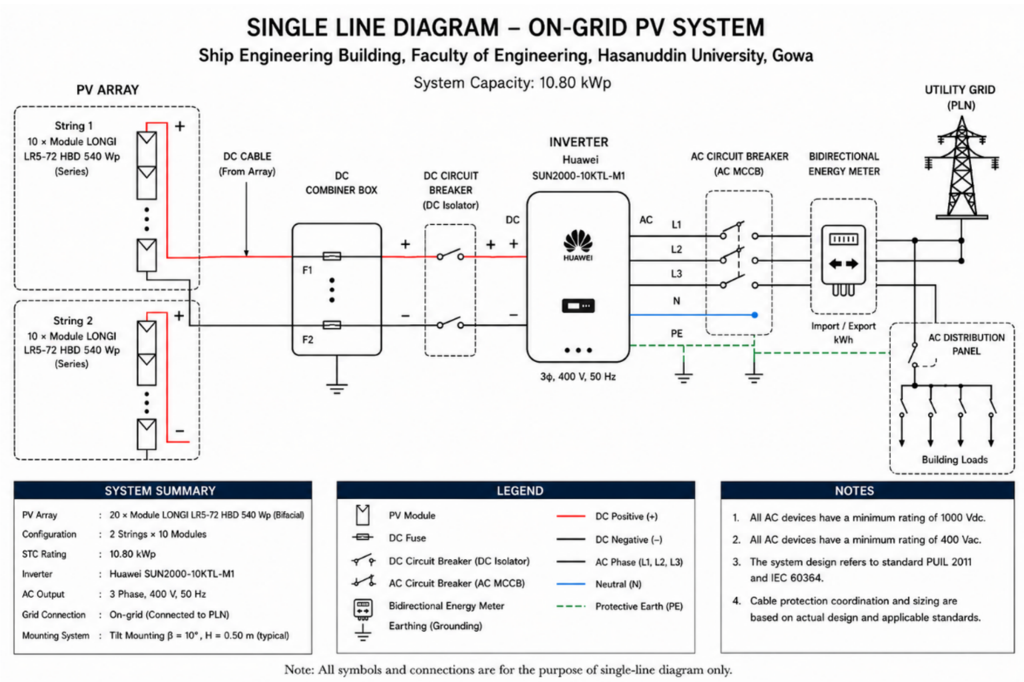

Figure 2. Single Line Diagram of the On-Grid PV System

3.3 Experimental Design and Simulation Parameters

The simulation uses PVsyst 7.3.1 with the 2D Unlimited Sheds model for bifacial systems. This model computes rear-side irradiance separately for three components: ground-reflected beam, ground-reflected diffuse, and direct sky diffuse. A bifaciality factor of $\varphi = 0.70$ is applied to the rear-side irradiance prior to energy conversion, consistent with the PVsyst model implementation described in Mermoud & Lejeune (2010) and further developed in version 7.x. The experimental design is a full factorial of 5 × 4 = 20 variants: tilt angle 5°, 10°, 15°, 20°, 25°; height above the roof (H) 0.30, 0.50, 0.80, 1.00 m.

Parameters held constant across all 20 simulations: pitch = 4.00 m (selected as a representative scenario; this choice is not the result of pitch optimization and is an acknowledged limitation — the implications of pitch variation are discussed in Section 4.4); number of sheds = 5; modules per row = 3; azimuth = 0° (facing North, optimal for a southern latitude); albedo = 0.25 (except in the sensitivity simulations). The Ground Coverage Ratio (GCR) is computed as:

$$GCR = w / p \quad (7)$$

where w is the projected module width per row (m) and p is the inter-row pitch (m) (IEC, 2021). The value of w is obtained from $w = L\_module \times \cos(\beta\_ref) = 2.278 \text{ m} \times \cos(5°) = 2.269 \text{ m} \approx 2.27 \text{ m}$, using the minimum tilt within the tested range (5°) as a conservative reference for the fixed-pitch calculation. For this configuration, GCR = 2.27/4.00 = 0.568 (56.8%). The recorded output parameters are: E_grid (kWh/year), Yf (kWh/kWp/year), PR, BPR, BG (%), VF Loss (%), and Near-shading Loss (%). An illustration of the design parameter space — covering system geometry, irradiance components, tilt angle, and mounting height — is shown in Figure 3, with the complete set of 20 scenarios, together with their simulation outputs, tabulated in Table 1 (Section 4.1)..

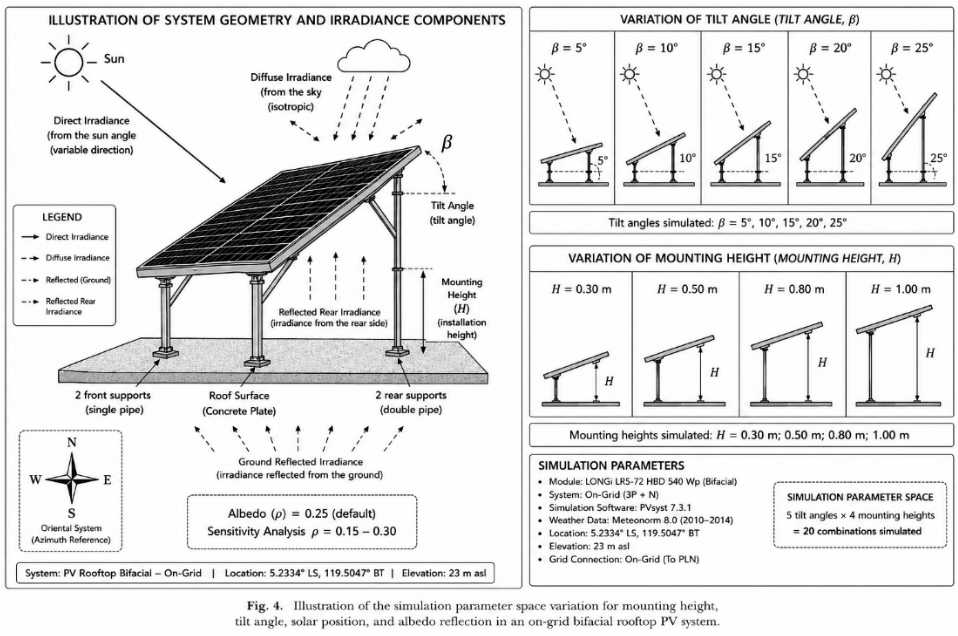

Figure 3. Illustration of the Simulation Parameter Space: System Geometry, Irradiance Components, Tilt Angle, and Mounting Height

3.4 Albedo Sensitivity Analysis

An albedo sensitivity analysis was performed at the optimal configuration (Tilt 10°, H = 1.00 m) using four values: 0.15 (waterproofing membrane/dark roof); 0.20 (weathered concrete, poor condition); 0.25 (standard weathered concrete, baseline); and 0.30 (relatively new concrete). This range was selected based on typical albedo values for concrete roofing materials in tropical climates (Ineichen et al., 1990; Andrews & Pearce, 2013). Albedo values above 0.30 were not examined because they lie outside the typical condition of building rooftop concrete surfaces and would require field measurement for verification.

3.5 Model Plausibility: Verification against the Literature and Statement of Uncertainty

This study is a purely simulation-based study without field validation. This statement is a key limitation that readers must understand: the reported numerical values (E_grid, PR, BG, etc.) reflect the output of the PVsyst 7.3.1 model and cannot be claimed as empirically accurate without field confirmation. The plausibility check performed here serves solely to confirm that the simulated values fall within a physically reasonable range, not as a substitute for validation.

The plausibility-verification approach used is as follows: the simulated PR values (0.852–0.872) were compared against PR ranges reported for grid-connected PV systems in tropical climates: Ademola and AlKassem (2025) reported a PR of 77–78% for a 500 kWp PV plant in Nigeria using PVsyst simulation; Mohamad Radzi et al. (2025) reported an overall PR of 82.9% (per-array range 56.3–86.7%) for a PV system in Kuala Lumpur, Malaysia (a more geographically comparable tropical climate). The simulated PR values in this study fall within a range consistent with these references, indicating no major anomaly in the simulation configuration. However, PR consistency with references from a different geographic setting does not validate the absolute BG or E_grid values.

The principal sources of uncertainty identified in this study are: (1) uncertainty in the Meteonorm 8.0 meteorological data (2010–2014 period data; Remund et al. (2020) report a Meteonorm GHI uncertainty of approximately 3–5% depending on location); (2) uncertainty in the actual albedo, which was not measured on site (the largest source based on the sensitivity analysis, a range of ±2.1% in E_grid for albedo 0.15–0.30); (3) uncertainty in φ (±0.8 pp in BG for $\varphi \pm 10\%$, based on the analytical estimate in Equation (6)); and (4) the limitations of the PVsyst 2D model, which does not capture 3D terrain effects or real-world installation irregularities. Overall, the authors estimate that the combined meteorological and albedo uncertainty could produce a deviation of actual E_grid from the simulated value on the order of 5–10%, an order-of-magnitude estimate that cannot be quantified more precisely without field data.

RESULTS AND DISCUSSION

4.1 Complete Simulation Results for 20 Scenarios

The simulation results for all 20 scenarios are presented in Table 1, grouped by mounting height (H = 0.30 m, 0.50 m, 0.80 m, and 1.00 m), each group comprising five tilt-angle variants (5°–25°). This grouping is intended to make the trend within each height group easier to read individually before cross-comparison in the following subsections. Figures 4 and 5 at the end of this subsection present a proportionally scaled visualization of the entire dataset for comparison across groups.

Table 1. Complete Simulation Results for the 20 Scenarios (Grouped by Mounting Height)

No.	Tilt (°)	H (m)	E_grid (kWh/yr)	Yf (kWh/kWp/yr)	PR	BPR	BG (%)	VF Loss (%)	Near Shade (%)
1	5°	0.30	17,197	1,592	0.852	0.819	3.8	-78.2	-0.1
2	10°	0.30	17,269	1,599	0.853	0.816	4.5	-74.8	-0.3
3	15°	0.30	17,215	1,594	0.854	0.812	5.1	-72.3	-0.8
4	20°	0.30	17,049	1,579	0.854	0.806	5.7	-70.7	-1.3
5	25°	0.30	16,779	1,554	0.853	0.801	6.5	-69.7	-2.0
6	5°	0.50	17,351	1,607	0.859	0.815	5.3	-69.6	-0.1
7	10°	0.50	17,407	1,612	0.860	0.812	5.8	-67.1	-0.3
8	15°	0.50	17,340	1,606	0.860	0.808	6.3	-65.8	-0.8
9	20°	0.50	17,156	1,588	0.859	0.803	6.8	-64.9	-1.3

No.	Tilt (°)	H (m)	E_grid (kWh/yr)	Yf (kWh/kWp/yr)	PR	BPR	BG (%)	VF Loss (%)	Near Shade (%)
10	25°	0.50	16,869	1,562	0.858	0.798	7.4	-64.8	-2.0
11	5°	0.80	17,521	1,622	0.868	0.809	7.0	-60.1	-0.1
12	10°	0.80	17,561	1,626	0.868	0.807	7.3	-58.5	-0.3
13	15°	0.80	17,479	1,618	0.867	0.804	7.7	-57.9	-0.8
14	20°	0.80	17,284	1,600	0.865	0.800	8.1	-58.1	-1.3
15	25°	0.80	16,984	1,573	0.863	0.795	8.6	-58.9	-2.0
16	5°	1.00	17,601	1,630	0.872	0.807	7.8	-55.6	-0.1
17	10°	1.00	17,631	1,633	0.871	0.805	8.0	-54.5	-0.3
18	15°	1.00	17,544	1,624	0.870	0.802	8.3	-54.3	-0.8
19	20°	1.00	17,344	1,606	0.868	0.798	8.7	-54.9	-1.3
20	25°	1.00	17,040	1,578	0.866	0.793	9.1	-56.0	-2.0

At the lowest mounting height (H = 0.30 m), E_grid peaks at tilt 10° (17,269 kWh/year) and decreases monotonically to tilt 25° (16,779 kWh/year, a difference of −490 kWh or −2.8%). Bifacial gain in this group falls within the lowest range among all height groups examined, from 3.8% (tilt 5°) to 6.5% (tilt 25°), because the rear-side view factor toward the ground remains limited at low mounting heights — VF Loss ranges from −69.7% to −78.2%, considerably larger (worse) than the other height groups discussed below.

At H = 0.50 m, the same pattern recurs: E_grid still peaks at tilt 10° (17,407 kWh/year). Compared with the H = 0.30 m group at the same tilt, E_grid rises by 138 kWh (+0.8%) and BG increases from 4.5% to 5.8% (+1.3 pp). This improvement is consistent with VF Loss improving from −74.8% to −67.1%, indicating that a height increase of just 0.20 m already produces a measurable improvement in the rear-side view factor, even though the E_grid-versus-tilt trend still follows the same tilt-10° peak pattern as the previous group.

At H = 0.80 m, the peak E_grid rises to 17,561 kWh/year (tilt 10°), an increase of 292 kWh (+1.7%) compared with H = 0.30 m at the same tilt. BG at the optimal configuration rises to 7.3%, nearly double the value at H = 0.30 m (4.5%). VF Loss improves significantly to −58.5%, confirming that raising the height from 0.50 m to 0.80 m yields a larger view-factor improvement than raising it from 0.30 m to 0.50 m — indicating that the relationship between height and BG is not fully linear over this range.

At the maximum height examined (H = 1.00 m), E_grid reaches its highest value among all 20 scenarios: 17,631 kWh/year at tilt 10°, with BG = 8.0% — nearly double the BG at H = 0.30 m for the same tilt. VF Loss improves to −54.5%, the best value among all height groups. The tilt-10° optimum for E_grid remains consistent across all four height groups, while the maximum BG is instead reached at tilt 25° (9.1%) — confirming the trade-off between maximizing BG and maximizing E_grid, discussed further in Section 4.2.

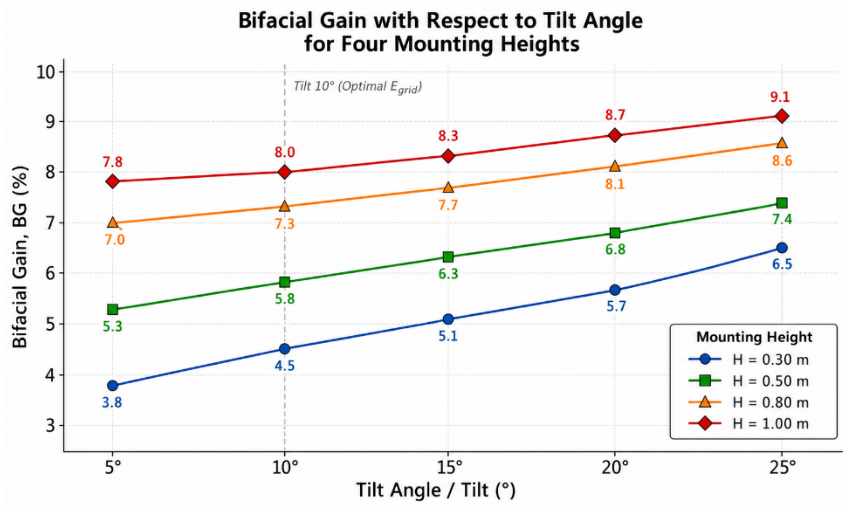

Figure 4. Bifacial Gain (%) versus Tilt Angle for Four Mounting Heights

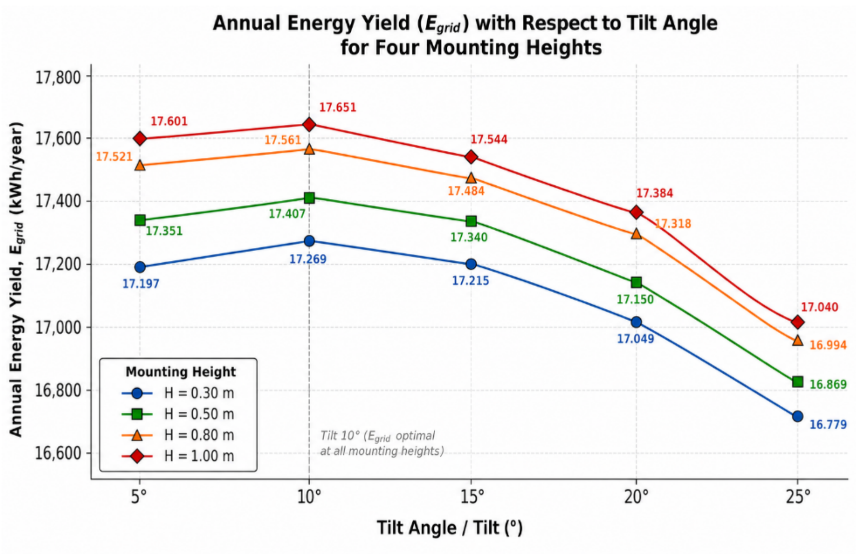

Figure 5. Annual Energy Yield E_Grid (kWh/year) versus Tilt Angle for Four Mounting Heights

4.2 Effect of Tilt Angle on E_grid and Bifacial Gain

The data in Table 1 show two consistent, opposing trends across all height groups. First, E_grid reaches its peak value at 10° tilt in all height groups, then decreases monotonically up to 25°. Second, BG increases monotonically with tilt angle across all heights. These two opposing trends reveal an inherent trade-off between BG and E_grid: maximizing BG is not equivalent to maximizing E_grid.

The decline in E_grid above tilt 10° is caused by two factors that can be verified from the data in Table 1: (1) near-shading loss increases from −0.3% (tilt 10°) to −2.0% (tilt 25°) across all heights; (2) irradiance on the collector plane decreases due to a less optimal angle-of-incidence geometry. The 10° optimal tilt aligns with low-latitude solar-irradiance theory (Hegedus & Luque, 2011): the theoretical optimal angle ranges from the site latitude up to 1.5× the latitude, i.e., 5.2°–7.8° for a latitude of 5.23°S, placing the 10° tilt at the upper bound of this range. The 10° tilt tested by Khoo et al. (2014) in Singapore (latitude 1.3°N, one of the four discrete angles they compared: 10°/20°/30°/40°) showed competitive irradiance, qualitatively consistent with the results of this study — although it should be noted that the main finding of that study actually highlighted the advantage of east-facing orientation, not a low tilt angle. That this study's results are consistent with the existing literature is an indication of simulation plausibility, not a weakness in novelty — this consistency is what lends confidence to the resulting design recommendations.

The increase in BG with rising tilt is explained by two mechanisms identifiable from the data in Table 1 (H = 0.30 m and H = 1.00 m subsets): (1) improvement in the geometric rear-side view factor toward the ground, consistent with Equation (4) and the Appelbaum & Bany (1979) model: VF Loss improves from −78.2% (tilt 5°) to −69.7% (tilt 25°) at H = 0.30 m; and (2) an increase in the sky-diffuse component received by the rear side as the angle increases, which is particularly relevant in humid tropical climates with a higher diffuse fraction (Deline et al., 2020).

4.3 Effect of Mounting Height on Bifacial Gain and E_grid

Increasing height from 0.30 m to 1.00 m produces a consistent BG increase at all tilt angles. At tilt 10° (the E_grid-optimal configuration): BG rises from 4.5% to 8.0% (+3.5 pp), accompanied by an E_grid increase of 362 kWh/year (+2.1%). The main mechanism is the view-factor improvement per Equation (5): VF Loss improves from −74.8% (H = 0.30 m) to −54.5% (H = 1.00 m) — a 20.3 pp improvement — yielding more ground-reflected irradiance reaching the rear side, consistent with the Appelbaum & Bany (1979) model and the findings of Sun et al. (2018).

Table 2. Effect of Mounting Height at the Optimal Tilt Configuration (10°)

H (m)	ΔH vs H=0.30 m	E_grid (kWh/yr)	ΔE_grid vs H=0.30	PR	BG (%)	VF Loss (%)
0.30	— (reference)	17,269	— (reference)	0.853	4.5	-74.8
0.50	+0.20 m	17,407	+138 kWh (+0.8%)	0.860	5.8	-67.1
0.80	+0.50 m	17,561	+292 kWh (+1.7%)	0.868	7.3	-58.5
1.00	+0.70 m	17,631	+362 kWh (+2.1%)	0.871	8.0	-54.5

4.4 Near-Shading Loss: Model Behavior Verification and Pitch-Variation Impact Estimate

The data in Table 1 confirm that near-shading loss is identical across all heights for each given tilt: −0.1% (5°); −0.3% (10°); −0.8% (15°); −1.3% (20°); −2.0% (25°). This confirms the documented behavior of PVsyst's 2D Unlimited Sheds model (Mermoud & Lejeune, 2010); inter-row shadow projection in the 2D model depends only on tilt and pitch, not on panel height. The practical implication is that, within the PVsyst 2D simulation framework, panel height can be optimized independently of near-shading considerations. In real installations, 3D effects, roof slope, and terrain irregularities may cause deviations from this model behavior.

The implications of pitch variation for near-shading loss can be estimated qualitatively from the geometric model. For the tilt-10° configuration with a baseline pitch of 4.00 m (GCR = 0.568; near-shading loss = −0.3%), reducing the pitch by 20% to 3.20 m would raise the GCR to 0.710, whereas increasing the pitch to 4.80 m would lower the GCR to 0.473. Because near-shading loss in unlimited-sheds-type PV systems increases monotonically with GCR for a given tilt and meteorology (Appelbaum & Bany, 1979; Deline et al., 2020), a shorter pitch configuration would produce higher near-shading loss, and vice versa. The magnitude of the change in near-shading loss resulting from pitch variation cannot be quantified analytically without PVsyst simulation, because it depends on the sun-angle distribution specific to this location; a quantitative estimate would require additional simulation, which is recommended for future research. Qualitatively, the conclusion that tilt 10° maximizes E_grid is likely robust to moderate pitch variation, because the mechanisms causing the E_grid decline above tilt 10° (near-shading loss and reduced frontal irradiance) do not depend on the absolute pitch value.

4.5 Albedo Sensitivity Analysis and Discussion of Non-Linearity

Table 3 presents the results of the albedo sensitivity analysis at the optimal configuration (Tilt 10°, H = 1.00 m). A disproportionate response pattern is identified: the BG increase per +0.05 albedo step is +1.0 pp (0.15→0.20), +0.9 pp (0.20→0.25), and +2.2 pp (0.25→0.30).

Table 3. Sensitivity of Bifacial Gain and E_grid to Albedo (Tilt 10°, H = 1.00 m)

Albedo	Surface Description	E_grid (kWh/yr)	ΔE_grid vs albedo 0.25	BG (%)	ΔBG per +0.05	PR
0.15	Waterproofing membrane / dark roof	17,267	−364 kWh (−2.1%)	6.1	— (baseline)	0.866
0.20	Weathered concrete, poor condition	17,451	−180 kWh (−1.0%)	7.1	+1.0 pp	0.869
0.25	Standard weathered concrete (baseline)	17,631	— (reference)	8.0	+0.9 pp	0.871
0.30	Relatively new / bright concrete	17,812	+181 kWh (+1.0%)	10.2	+2.2 pp	0.874

The larger BG increase (+2.2 pp) over the 0.25→0.30 albedo interval, compared with the preceding intervals (+0.9–1.0 pp), needs to be interpreted with caution for several important reasons.

First, based on Equation (5): G_rear,ground = ρ × G_H × VF_rear→ground, the relationship between G_rear,ground and ρ is linear if G_H and VF_rear→ground are constant. However, in the PVsyst 2D model, the G_H used in the calculation is not identical across all simulations, because it depends on the irradiance component received at the ground, which can change indirectly depending on albedo (although this effect is minor in the one-way model). The more significant non-linearity arises from the fact that VF_rear→ground itself is a non-linear function of geometry, so the absolute BG response to changes in ρ need not be linear. This is consistent with the non-linearity reported by Deline et al. (2020) for a different configuration.

Critical note that readers must understand: The authors did not perform a per-component Loss Diagram decomposition (Ground Reflected Beam vs. Ground Reflected Diffuse vs. Sky Diffuse on Rear) for each albedo value in this study. Consequently, no more specific mechanistic claim about the cause of the +2.2 pp jump can be made. This observation is reported as simulation data that requires further investigation through Loss Diagram decomposition and field confirmation, not as a verified mechanistic finding. The BG value of 10.2% at albedo 0.30 must be interpreted with heightened caution, as it lies at the upper bound of the range examined.

The practical implication for PV system designers is that the high sensitivity of BG to albedo (a range of 4.1 pp for albedo variation 0.15–0.30) shows that measuring actual albedo at the installation site significantly improves the accuracy of energy-production estimates. Assuming an albedo value without field measurement is the largest source of uncertainty in rooftop bifacial system design.

4.6 Optimal Configuration and Design Implications

Two optimal configurations are identified based on different criteria. To maximize E_grid: Tilt 10° + H = 1.00 m yields E_grid = 17,631 kWh/year, PR = 0.871, BPR = 0.805, BG = 8.0%, Yf = 1,633 kWh/kWp/year. To maximize BG: Tilt 25° + H = 1.00 m yields BG = 9.1%, but a lower E_grid (17,040 kWh/year) due to the dominance of a −2.0% near-shading loss.

From a systems-engineering perspective, the Tilt 10° + H = 1.00 m configuration is recommended. Increasing height from 0.30 m to 1.00 m provides an additional 362 kWh/year (+2.1%) in energy at the cost of higher mounting expense — an economic feasibility analysis (LCOE, payback period) relating to the additional mounting cost was not examined in this study and is recommended as a priority for future research before implementation.

4.7 Comparison with Prior Research

The 10° tilt obtained in this study falls within the range of angles tested by Khoo et al. (2014) in Singapore (10°/20°/30°/40°, although that study did not test 5° and its main finding was the advantage of east-facing orientation rather than low tilt) and is consistent with low-latitude solar-irradiance theory (Hegedus & Luque, 2011). The BG values obtained in this study (3.8–9.1% at albedo 0.25) are qualitatively consistent with the bifacial-gain range reported for fixed-tilt systems in the global study by Rodríguez-Gallegos et al. (2020) at low albedo (0.20–0.25). The BG value at H = 1.00 m (8.0%) lies at the upper bound of the range projected by Sun et al. (2018) (below 10% for albedo 0.25 at the global scale), which is consistent with the humid tropical climate conditions in South Sulawesi with GHI = 1,855 kWh/m²/year — a higher GHI yields more ground irradiance available for reflection to the rear side, increasing G_rear,ground per Equation (5). This quantitative difference, although qualitatively consistent with the understood mechanism, cannot be confirmed as a GHI effect alone without an experimental control that isolates the GHI variable from other variables.

CONCLUSION

This study presents a PVsyst 7.3.1 simulation-based parametric analysis of 20 combinations of tilt angle (5°–25°) and mounting height (0.30–1.00 m) for a 10.8 kWp rooftop bifacial PV system in South Sulawesi (5.2334°S, 119.5047°E), using Meteonorm 8.0 data with an annual GHI of 1,855 kWh/m²/year. The simulation consistently shows that a 10° tilt angle maximizes annual energy yield (E_grid) across all mounting heights, with the optimum configuration obtained at H = 1.00 m, producing E_grid = 17,631 kWh/year, PR = 0.871, BPR = 0.805, and BG = 8.0%. This result is consistent with low-latitude solar-irradiance theory (Hegedus & Luque, 2011) and field measurements reported for similar tropical climates (Khoo et al., 2014). Although bifacial gain continues to increase with larger tilt angles, the corresponding increase in near-shading loss and reduction in front-side irradiance cause annual energy production to decline beyond the 10° optimum.

Increasing the mounting height from 0.30 m to 1.00 m significantly improves bifacial performance through an enhanced rear-side view factor, consistent with the Appelbaum and Bany (1979) model. At the optimal tilt angle, this increase raises BG by 3.5 percentage points and E_grid by 362 kWh/year (+2.1%), while near-shading loss remains unaffected within the PVsyst 2D Unlimited Sheds model. The separate albedo sensitivity analysis further indicates that BG varies from 6.1% to 10.2% for albedo values between 0.15 and 0.30, demonstrating that rooftop surface reflectance is one of the dominant factors influencing bifacial PV performance. The larger BG increase observed at the 0.25→0.30 albedo interval is reported as a simulation result qualitatively consistent with the non-linear behavior described by Deline et al. (2020), although its underlying mechanism requires further investigation.

Overall, a 10° tilt angle combined with a 1.00 m mounting height is recommended for rooftop bifacial PV installations under the humid tropical climate of South Sulawesi because it provides the best balance between annual energy yield and bifacial performance. The parametric dataset generated in this study offers practical engineering guidance for rooftop bifacial PV design in similar tropical regions. Nevertheless, the results should be interpreted within the limitations of a simulation-based study, including the absence of field validation, the use of Meteonorm 8.0 meteorological data (2010–2014), and a fixed inter-row pitch. Future research should therefore focus on field validation, updated meteorological datasets, economic feasibility assessment, pitch optimization, and broader geographical applications to further improve the reliability and applicability of the proposed design recommendations.

REFERENCES

Ademola, A. S., & AlKassem, A. (2025). Analytical design and hybrid techno-economic assessment of grid-connected PV system for sustainable development. Processes, 13(11), Article 3412. https://doi.org/10.3390/pr13113412

Andrews, R. W., & Pearce, J. M. (2013). The effect of spectral albedo on amorphous silicon and crystalline silicon solar photovoltaic device performance. Solar Energy, 91, 233–241. https://doi.org/10.1016/j.solener.2013.01.030

Appelbaum, J., & Bany, J. (1979). Shadow effect of adjacent solar collectors in large scale systems. Solar Energy, 23(6), 497–507. https://doi.org/10.1016/0038-092X(79)90073-2

Asgharzadeh, A., Marion, B., Deline, C., Hansen, C., Stein, J. S., & Toor, F. (2018). A sensitivity study of the impact of installation parameters and system configuration on the performance of bifacial PV arrays. IEEE Journal of Photovoltaics, 8(3), 798–805. https://doi.org/10.1109/JPHOTOV.2018.2819676

Deline, C., Ayala Pelaez, S., MacAlpine, S., & Olalla, C. (2020). Estimating and parameterizing mismatch power loss in bifacial photovoltaic systems. Progress in Photovoltaics: Research and Applications, 28(7), 691–703. https://doi.org/10.1002/pip.3259

Hegedus, S., & Luque, A. (2011). Handbook of photovoltaic science and engineering (2nd ed.). John Wiley & Sons. https://doi.org/10.1002/9780470974704

Ineichen, P., Guisan, O., & Perez, R. (1990). Ground-reflected radiation and albedo. Solar Energy, 44(4), 207–214. https://doi.org/10.1016/0038-092X(90)90149-7

International Electrotechnical Commission. (2019). IEC TS 60904-1-2:2019: Photovoltaic devices – Part 1-2: Measurement of current-voltage characteristics of bifacial photovoltaic (PV) devices. IEC.

International Electrotechnical Commission. (2021). IEC 61724-1:2021: Photovoltaic system performance – Part 1: Monitoring. IEC.

International Energy Agency. (2022). Solar PV global supply chains. IEA.

Khoo, Y. S., Nobre, A., Malhotra, R., Yang, D., Rüther, R., Reindl, T., & Aberle, A. G. (2014). Optimal orientation and tilt angle for maximizing in-plane solar irradiation for PV applications in Singapore. IEEE Journal of Photovoltaics, 4(2), 647–653. https://doi.org/10.1109/JPHOTOV.2013.2292743

Kopecek, R., & Libal, J. (2021). Bifacial photovoltaics 2021: Status, opportunities and challenges. Energies, 14(8), Article 2076. https://doi.org/10.3390/en14082076

Marion, B., MacAlpine, S., Deline, C., Asgharzadeh, A., Toor, F., Riley, D., Stein, J., & Hansen, C. (2017). A practical irradiance model for bifacial PV modules. In Proceedings of the IEEE 44th Photovoltaic Specialist Conference (PVSC) (pp. 1537–1543). IEEE. https://doi.org/10.1109/PVSC.2017.8366263

Mermoud, A., & Lejeune, T. (2010). Performance assessment of a simulation model for PV modules of any available technology. In Proceedings of the 25th European Photovoltaic Solar Energy Conference (EU PVSEC). Valencia, Spain.

Mohamad Radzi, P. N. L., Mekhilef, S., Mohamed Shah, N., Akhter, M. N., Hassani, S., Albaker, A., & Wahyudie, A. (2025). Performance evaluation and degradation analysis of grid connected photovoltaic systems for energy efficient buildings in tropical climates. Scientific Reports, 15, Article 39103. https://doi.org/10.1038/s41598-025-26765-9

Remund, J., Muller, S., Kunz, S., Huguenin-Landl, B., Studer, C., & Cattin, R. (2020). Meteonorm version 8 handbook – Part II: Theory. Meteotest AG.

Rodríguez-Gallegos, C. D., Liu, H., Gandhi, O., Singh, J. P., Krishnamurthy, V., Kumar, A., Stein, J. S., Wang, S., Li, L., Reindl, T., & Peters, I. M. (2020). Global techno-economic performance of bifacial and tracking photovoltaic systems. Joule, 4(7), 1514–1541. https://doi.org/10.1016/j.joule.2020.05.005

Sun, X., Khan, M. R., Deline, C., & Alam, M. A. (2018). Optimization and performance of bifacial solar modules: A global perspective. Applied Energy, 212, 1601–1610. https://doi.org/10.1016/j.apenergy.2017.12.041